

Enhanced sensing of non-Newtonian effects at ultrashort range with exceptional points in optomechanical systems*

Jian Liu, Lei Chen, and Ka-Di Zhu[†]

*Key Laboratory of Artificial Structures and Quantum Control (Ministry of Education),
School of Physics and Astronomy, Shanghai Jiao Tong University,
800 DongChuan Road, Shanghai 200240, China,*

Collaborative Innovation Center of Advanced Microstructures, Nanjing, China

(Dated: November 27, 2024)

We propose an optomechanical nano-gravimeter based on exceptional points. The system is a coupled cavity optomechanical system, in which the gain and loss are applied by driving the cavities with a blue detuned and red detuned electromagnetic field, respectively. When the gain and loss reach a balance, the system will show the degeneracy of exceptional points, and any perturbation will cause an eigenfrequencies split, which is proportional to the square root of the perturbation strength. Compared with the traditional optomechanical sensors, the sensitivity is greatly enhanced. This work paves the way for the design of optomechanical ultrasensitive force sensors that can be applied to detect non-Newtonian effects, high-order weak interactions, and so on.

I. INTRODUCTION

In quantum mechanics and quantum optics, most systems are open and exchange energy or particles with the surrounding environment. The dynamics of this open quantum system can be described by non-Hermitian Hamiltonian with complex eigenvalues. It has been proved that parity-time (PT) symmetrical non-Hermitian Hamiltonian can also have a real eigenvalue spectrum[1], providing a new design scheme for devices with novel functions[2-4]. Depending on the real or complex nature of the eigenvalues of the Hamiltonian, the system can change from PT-symmetric to PT-broken phase at the exceptional points (EPs). The physical existence of EPs has been proven through many experiments in some different systems, for example, nanomechanical resonator[5], optical microcavities[6], photonic lattices[7]. In such systems, two or more eigenmodes coalesce at the EPs, leading to a variety of unconventional effects observed in experiments, such as loss-induced transparency[8], unidirectional lasing[9], topological chirality[10], exotic topological states[11], and chaos[12].

Recently, it has been shown that the complex-square-root topology near the second-order EPs can enhance the sensitivity of an optical system to the external perturbation[13,14]. If a higher-order EP is used (greater than the second-order), this can in principle further amplify the frequency shift induced by the perturbations, resulting in higher sensitivity[15]. A growing number of theoretical and experimental studies have been devoted to such applications[16,17].

On the other hand, some recent theories of physics beyond the standard model point to the possibility of new physics related to gravity. Those theories that attempt to unify the standard model with gravity, predict the

existence of extra dimensions, exotic particles, or light moduli in string theory that could cause a mass coupling in addition to the Newtonian gravitational potential at short distances[18]. The Yukawa potential due to new interactions is typically taken to modify the gravitational inverse square law

$$V(r) = -G_N \frac{m_t m_s}{r} (1 + \alpha e^{-r/\lambda}), \quad (1)$$

where G_N is Newton's constant, m_t and m_s are the test mass and source mass respectively, r is the center of mass separation, and α is the strength of any new effect with a length scale of λ . Many experimental and theoretical schemes are dedicated to detecting gravity deviations at short distances[19-22]. Among these different systems, benefiting from the high mechanical quality factor properties and the all-optical-domain methods without heat effect and energy loss caused by circuits, in recent years, the nano-optomechanical systems have played an important role in the application of quantum limit detection, including force[23,24], mass[25], displacement[26] and so on.

However no matter which system is used, force-sensing are mainly based on the mechanism of linear dependent between the force and displacement[23] or the force and the resonance frequency[24]. Here we demonstrate an alternative force-sensing scheme that can operate at non-Hermitian spectral degeneracies (known as the exceptional point), thereby increasing the sensitivity of the optical system. Our proposal is based on two mechanically coupled optomechanical resonators which are placed in two optical cavities respectively. The cavities are driven with blue-detuned and red-detuned laser, respectively. At the balance between gain and loss, the system features an EP in its mechanical spectrum. Any variation of force gradient will perturb the system from its exceptional point, leading to frequency splitting. The sensitivity enhancement more than 10^6 was theoretically demonstrated with a sensor operating at exceptional points.

*

[†] zhukadi@sjtu.edu.cn

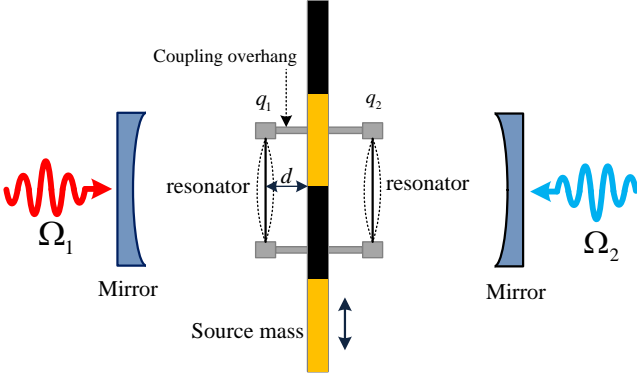


FIG. 1. Generic setup. A coupled cavity optomechanical system with double resonators. A source mass with varying density sections is positioned in the middle. The two cavities are driven by blue- and red-detuned laser, respectively.

II. THEORY FRAMEWORK

Let us consider a coupled cavity optomechanical system with double resonators. A schematic of our setup is sketched in Fig. 1, where two mechanical resonators are coupled to two cavities respectively, and simultaneously coupled to each other. There is a source mass with varying density sections positioned between the two cavities with the same separation d from each resonator. The two cavities are driven by blue- and red-detuned laser fields, respectively. The Hamiltonian of the optical controlled mechanical gain/loss optomechanical systems can be expressed as ($\hbar = 1$).

$$H = \sum_{j=1,2} [\Delta_j c_j^\dagger c_j + \omega_j (q_j^2 + p_j^2) - g_0 c_j^\dagger c_j q_j] - J q_1 q_2 + \sum_{j=1,2} (\Omega_j c_j^\dagger + H.c.), \quad (2)$$

where ω_j is the resonance frequency of j th resonator, Δ_j is the frequency detuning between the j th cavity mode and the j th external driving field. The first term denotes two cavity modes, two mechanical modes and the optomechanical coupling g_0 between them, the second term corresponds the coupling J between the mechanical resonators and the third term represents the two driving lasers with strengths Ω_i .

The dynamics of the cavity fields and resonators can be described by quantum Langevin equations. We can neglect the fluctuations of the cavity fields and mechanical resonators in the strong external driving condition and from Eq.(2) we can get the equations of motion for the mechanical modes without explicit optical coupling

$$\frac{d}{dt} p_1 = -(\omega_1 + \delta\omega_1) q_1 + J q_2 - (\Gamma_1 + \gamma_1) p_1, \quad (3)$$

$$\frac{d}{dt} p_2 = -(\omega_2 + \delta\omega_2) q_2 + J q_1 - (\Gamma_2 + \gamma_2) p_2, \quad (4)$$

where the optically induced mechanical frequency shift and damping rate are [27],

$$\delta\omega_j = 2g_0^2 n_{cav}^{(j)} \left[\frac{\Delta_j - \omega_j}{(\kappa_j/2)^2 + (\Delta_j - \omega_j)^2} + \frac{\Delta_j + \omega_j}{(\kappa_j/2)^2 + (\Delta_j + \omega_j)^2} \right], \quad (5)$$

$$\Gamma_j = g_0^2 n_{cav}^{(j)} \kappa_j \left[\frac{-1}{(\kappa_j/2)^2 + (\Delta_j - \omega_j)^2} + \frac{1}{(\kappa_j/2)^2 + (\Delta_j + \omega_j)^2} \right]. \quad (6)$$

Here $n_{cav}^{(j)}$ represent the photon number circulating inside the j th cavity, κ_j is the j th overall cavity intensity decay rate. With the optical controlling on mechanical properties, we can obtain PT symmetrical systems through the cavity optomechanical effects.

With the simplification, we use two identical optical cavities and resonators, that means $\omega_j (j = 1, 2) = \omega_m$, $\kappa_j (j = 1, 2) = \kappa$. We use the same driving laser to drive both optical cavities simultaneously, $\Delta_j (j = 1, 2) = \Delta$, $n_{cav}^{(j)} (j = 1, 2) = n_{cav}$. Thereby $\delta\omega_j (j = 1, 2) = \delta\omega_m$, $\Gamma_j (j = 1, 2) = \Gamma_m$. When $\gamma_{eff} = -(\Gamma_m + \gamma_1) = \Gamma_m + \gamma_2$, one can get the dynamical equations for the coupled optomechanical resonators with PT symmetry

$$\frac{d}{dt} q_1 = \omega_{eff} p_1, \quad (7)$$

$$\frac{d}{dt} q_2 = \omega_{eff} p_2, \quad (8)$$

$$\frac{d}{dt} p_1 = -\omega_{eff} q_1 + J q_2 + \gamma_{eff} p_1, \quad (9)$$

$$\frac{d}{dt} p_2 = -\omega_{eff} q_2 + J q_1 - \gamma_{eff} p_2, \quad (10)$$

Here the effective resonator frequency $\omega_{eff} = \delta\omega + \omega_m$. Now, let us derive expressions describing the physical properties of the boundary between the broken- and unbroken-PT -symmetry regions. Eqs.(7)–(10) can be rewritten in a compact matrix form as

$$i \frac{d}{dt} |\Psi\rangle = H_{eff} |\Psi\rangle, \quad (11)$$

with $|\Psi\rangle = (q_1, p_1, q_2, p_2)^T$, and the effective Hamiltonian

$$H_{eff} = i \begin{pmatrix} 0 & \omega_{eff} & 0 & 0 \\ -\omega_{eff} & \gamma_{eff} & J & 0 \\ 0 & 0 & 0 & \omega_{eff} \\ J & 0 & -\omega_{eff} & -\gamma_{eff} \end{pmatrix}. \quad (12)$$

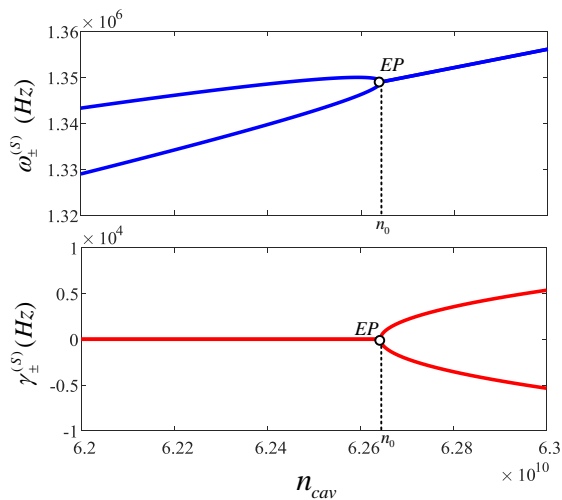


FIG. 2. Real(left) and imaginary(right) part of the mechanical eigenfrequency as a function of n_{cav} with $\Delta = \omega_m$.

The eigenvalues of the effective Hamiltonian H_{eff} are given as

$$\omega_{\pm} = \sqrt{\omega_{eff}^2 - \frac{\gamma_{eff}^2}{2}} \pm \sqrt{\left(\frac{\gamma_{eff}^2}{2}\right)^2 + \omega_{eff}^2(J^2 - \gamma_{eff}^2)}. \quad (13)$$

There are many types of optomechanical resonators. For illustrating, we choose one of them, in which the mechanical degree of freedom is a flexible, partially transparent object (such as a dielectric membrane) placed inside a Fabry-Perot cavity[28]. Here we use a commercial SiN membrane $1mm$ square by $50nm$ thick. To bridge the theoretical proposal and experiments, we use the following practical device parameters $\omega_m = 100kHz$, $\kappa = 10MHz$, $g_0 = 50Hz$. Tunable coupling of two vibrating mechanical resonators can be achieved by the piezoelectric effect or the photothermal effect[3] and the coupling rate $J = \kappa/100 = 0.1MHz$. We then set the cavity-pump detuning $\Delta = \omega_m$. Fig.2 shows that the PT-broken regime and the PT symmetric regime are separated by the exceptional point, where the eigenfrequencies coalesce. Here $\omega_{\pm}^{(S)} = \text{Re}(\omega_{\pm})$ and $\gamma_{\pm}^{(S)} = \text{Im}(\omega_{\pm})$ correspond to the frequencies and linewidths of the super modes. As n_{cav} increases, the frequencies of the pair of super modes approach to each other and coalesce, while the linewidths starts with zero and then branches, indicating that the PT symmetry is broken.

III. MEASUREMENT

In the following we propose a method for measuring the force gradient. In such experiments the Casimir effect is an unwanted background that needs to be suppressed. The “isoelectronic” or “Casimir-less” technique introduced firstly in Ref.[29] can be used to achieve this

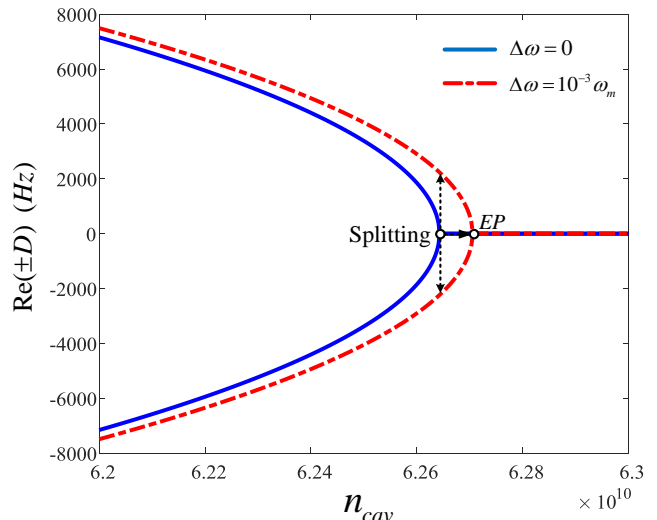


FIG. 3. Eigenfrequency difference of the effective mechanical system before perturbation (full blue lines) and after perturbation (dashed red lines) by variation of force gradient corresponding to a frequency shift of $\Delta\omega = 10^{-3}\omega_m$.

purpose. The mass source with $20mm$ square by $500nm$ thick is composed of alternating strips of different materials (e.g., Au and Si) as shown in Fig.1. In the absence of electromagnetic contributions, a comparison of the forces exerted on a test mass (resonator) by materials of different densities leads to constraints on α and λ of Eq. (1). When the mass source moves up and down, the change of forces exerted on the test mass can be regarded as the perturbation of the optomechanical system. The frequency shift is proportional to the variation of force gradient at the mass of center of the resonators.

$$\Delta\omega = -\frac{1}{2m_t\omega_m} \frac{\partial F}{\partial r}. \quad (14)$$

Thereby for an ordinary sensor, the induced frequency shift is proportional to the strength of the perturbation $\partial F/\partial r$.

An important parameter in a PT symmetrical system is the difference between the eigenfrequencies, namely the eigenfrequency splitting which can be defined as $D = \text{Re}(\omega_+ - \omega_-)$. We plot D as a function of n_{cav} in Fig. 3 by the blue line. At EP, both eigenvalues and eigenvectors are coalesce. If the system is subjected to a weak perturbation $\Delta\omega$, the eigenfrequency spectrum will be changed from $D(\omega_m)$ to $D(\omega_m + \Delta\omega)$. In the same figure, we show the eigenfrequency of the effective optomechanical system after the perturbation $\Delta\omega = 10^{-3}\omega_m$ appears with a dash red line. This perturbation can be caused by a variation in the force gradient of the resonators. From the figure we can see that the perturbation pushes the exceptional point to the right, and therefore the non-Hermitian degeneracy of the eigenfrequency is released at the exceptional point before the perturbation, which

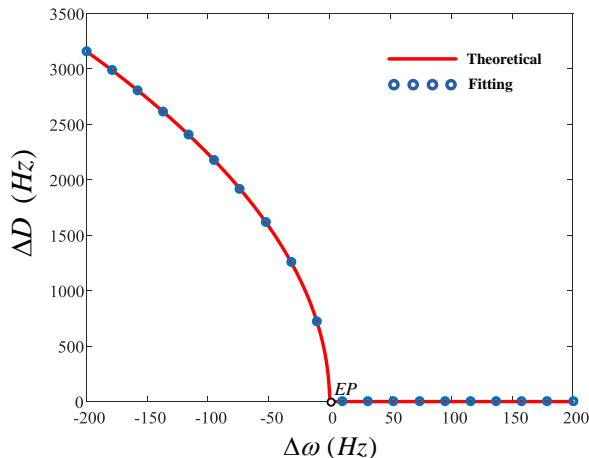


FIG. 4. Theoretical and fitting curves of super mode frequency splitting as a function of perturbation. The fitting expression is Eq.(15) with $Y = 5 \times 10^4$.

causes the super mode frequency to split. This splitting can be used as a signal of the non-Newtonian effect.

IV. SENSITIVITY

When we are trying to evaluate the sensitivity of the sensor at EP, we need to know the effect of frequency perturbations on the super mode frequency splitting near the EP ($n_0 \simeq 6.2643 \times 10^{10}$). Therefore, the sensitivity is defined as $\Delta D(\Delta\omega) = [D(\omega_m) - D(\omega_m + \Delta\omega)]|_{n_0}$. Fig.4 shows ΔD as a function of the perturbation $\Delta\omega$ at EP. We fit the curve numerically to get an equivalent expression

$$\Delta D \simeq \sqrt{Y\Delta\omega}. \quad (15)$$

Here the constant $Y = 5 \times 10^4$. It is not difficult to see that the eigenfrequency splitting near the EP point is proportional to the square root of the frequency perturbation $\Delta\omega$ that is, proportional to the square root of $\partial F/\partial r$. For a conventional sensor, the frequency change is linear dependence. Therefore due to the complex square root topology near the exception point, the eigenfrequency splitting is greatly enhanced for sufficiently small perturbations compared to sensors operating under non-exception point sensing schemes.

We can define the sensitivity enhancement factor η as the square root dependence on $\Delta\omega$ instead of a linear dependence, which can be given by $\eta = \Phi/\Delta\omega = \sqrt{Y/\Delta\omega}$. This equation shows that the sensitivity enhancement is inversely proportional to the square-root of the perturbation $\Delta\omega$. So η is greatly increased for weak perturbation, proving the efficiency of the EP sensor in detecting weak forces.

The resolution of the spectrum is determined by the full width at half maximum (FWHM) of the spectral

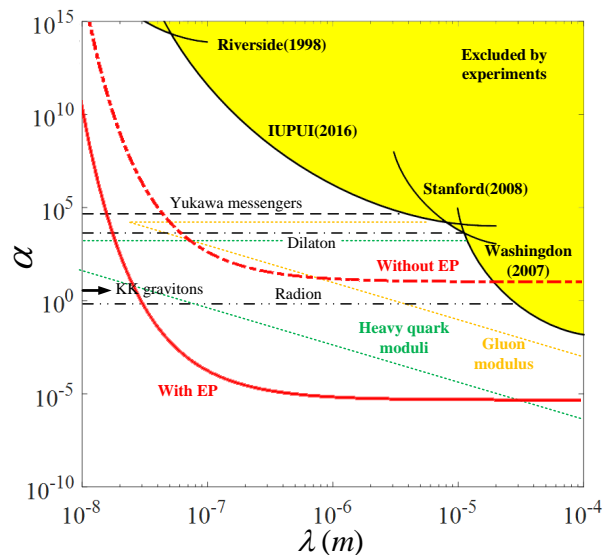


FIG. 5. Experimental constraints of short-range forces caused by Yukawa-type interaction potentials [19-22] and theoretical predictions of this work. The shaded region is excluded with 95% confidence level. The full line and dashed denote the results of EP measurement scheme and conventional optomechanical sensor respectively.

lines. The linewidth of the mechanical resonator in the optomechanical system can be calculated by

$$\sigma = \frac{\omega_n}{Q}. \quad (16)$$

The membrane have been measured $Q = 1.2 \times 10^7$ at $T = 300mK$ [28], then we can obtain $\sigma = 8.3mHz$, which is the smallest detectable frequency shift in traditional optomechanical spectrum. At the same time, due to various noise processes, the spectral lines will broaden[30]. Because the membrane has a high mechanical quality factor and meets low temperature conditions, the thermal noise of the system can be controlled at a level much lower than the line width. On the other hand, under high vacuum conditions(approximately $10^{-4}Pa$), the momentum exchange noise of the resonators can also be greatly reduced to a negligible level. The strength of the perturbation required to cause the same frequency shift in the EP system is smaller due to the complex square root topology. To compare ordinary sensors with EP-based sensors, we making $\Delta D = \sigma$ in Eq.(15). Thus we get $\Delta\omega_{\min} \sim 10^{-9}Hz$ (without EP is $8.3mHz$) and then we can obtain the force gradient resolution with Eq.(14), $(\partial F/\partial r)_{\min} = 2m_i\omega_m\Delta\omega_{\min} \sim 10^{-14}N/m$. In order to measure the interactions at ultra-short distances, we bring the membrane close enough to the mass source with a distance of $d = 100nm$. The mass source we use is a plate with a thickness of $500nm$, so the distance between the membrane and the center of the plate is $r = 375nm$. In these conditions, the force sensitivity of the EP scheme is at the level of $10^{-20}N$.

In Fig. 5 we describe the experimental constraints and theoretical prediction on the forces caused by the interaction potential of the Yukawa form [19-22]. The dashed line is the constraint from the conventional optomechanical sensor, and the full black line represents the result of the EP measurement scheme. It can be clearly seen that the EP-based optomechanical nanogravity gradiometer performs better. We hope that the proposed system can advance the search for non-Newtonian gravity by an enhanced sensitivity of $\eta = 6.4 \times 10^6$ compared with traditional optomechanical method and reach an unprecedented sensitivity for force sensing.

V. CONCLUSION

Based on cavity optomechanics we propose a high-efficiency optomechanical nano-gravimeter operating at exceptional points, non-Hermitian degeneracy. The sys-

tem consists of two mechanically coupled optomechanical resonators. The cavity is driven by a blue detuned (red detuned) laser to induce mechanical gain (loss). The system has an EP at the gain and loss balance, where any perturbation will cause a frequency split, which is proportional to the square root of the intensity of the perturbation. Hence, for a sufficiently small perturbation, the splitting at the exceptional point is larger compared to traditional optomechanical sensors. This particular characteristic of exceptional points has been proposed for use in weak short range force measurement.

ACKNOWLEDGMENTS

This work was supported by the National Natural Science Foundation of China (Nos.11274230 and 11574206), the Basic Research Program of the Committee of Science and Technology of Shanghai (No.14JC1491700).

-
- [1] C. M. Bender and S. Boettcher, Real spectra in non-Hermitian Hamiltonians having PT symmetry, *Phys. Rev. Lett.* **80**, 5243 (1998).
 - [2] L. Feng, R. El-Ganainy and L. Ge, Non-Hermitian photonics based on parity-time symmetry, *Nature Photonics* **11**, 752 (2017).
 - [3] X. W. Xu, Y. Liu, C. P. Sun, and Y. Li, Mechanical PT symmetry in coupled optomechanical systems, *Phys. Rev. A* **92**, 013852 (2015).
 - [4] Z. Y. Feng, J. W. Ma, and X. K. Sun, Parity-time-symmetric mechanical systems by the cavity optomechanical effect, *Opt. Lett.* **43**, 4088 (2018).
 - [5] B. Peng, Ş. K. Özdemir, M. Liertzer, W. Chen, J. Kramer, H. Yilmaz, J. Wiersig, S. Rotter and L. Yang, Chiral modes and directional lasing at exceptional points, *Proc. Natl. Acad. Sci. USA* **113**, 6845–6850 (2016).
 - [6] S. B. Lee, J. Yang, S. Moon, S. Y. Lee, J. B. Shim, S. W. Kim, J. H. Lee and K. An, Observation of an exceptional point in a chaotic optical microcavity, *Phys. Rev. Lett.* **103**, 134101 (2009).
 - [7] C. Hahn, Y. Choi, J. W. Yoon, S. H. Song, C. H. Oh and P. Berini, Observation of exceptional points in reconfigurable non-Hermitian vector-field holographic lattices, *Nat. Commun.* **7**, 12201 (2016).
 - [8] B. Peng, S. K. Özdemir, S. Rotter, H. Yilmaz, M. Liertzer, F. Monifi, C. M. Bender, F. Nori, and L. Yang, Loss-induced suppression and revival of lasing, *Science* **346**, 328 (2014).
 - [9] S. Longhi and L. Feng, Unidirectional lasing in semiconductor microring lasers at an exceptional point, *Photonics Research*, **5**, 11–16 (2017).
 - [10] H. Xu, D. Mason, L. Jiang and J. G. E. Harris, Topological energy transfer in an optomechanical system with exceptional points, *Nature* **537**, 80–83 (2016).
 - [11] H. Zhou, C. Peng, Y. Yoon, C. W. Hsu, K. A. Nelson, L. Fu, J. D. Joannopoulos, M. Soljačić, and B. Zhen, Observation of bulk Fermi arc and polarization half charge from paired exceptional points, *Science* **359**, 1009 (2018).
 - [12] X. Y. Lü, H. Jing, J. Y. Ma and Y. Wu, PT-symmetry-breaking chaos in optomechanics, *Phys. Rev. Lett.* **114**, 253601 (2015).
 - [13] W. Chen, Ş. K. Özdemir, G. Zhao, J. Wiersig and L. Yang, Exceptional points enhance sensing in an optical microcavity, *Nature* **548** 192–196 (2017).
 - [14] P. Djourjoe, Y. Pennec and B. Djafari-Rouhani, Exceptional Point Enhances Sensitivity of Optomechanical Mass Sensors, *Phys. Rev. Appl.* **12**, 024002 (2019).
 - [15] H. Hodaei, A. U. Hassan, S. Wittek, H. Garcia-Gracia, R. El-Ganainy, D. N. Christodoulides and M. Khajavikhan, Enhanced sensitivity at higher-order exceptional points, *Nature* **548**, 187–191 (2017).
 - [16] Ş. K. Özdemir, S. Rotter, F. Nori and L. Yang, Parity-time symmetry and exceptional points in photonics, *Nature Materials* **18**, 783–798 (2019).
 - [17] J. Wiersig, Sensors operating at exceptional points: General theory, *Phys. Rev. A* **93**, 033809 (2016).
 - [18] S. Dimopoulos and A. A. Geraci, Probing submicron forces by interferometry of Bose-Einstein condensed atoms, *Phys. Rev. D* **68**, 124021 (2003).
 - [19] U. Mohideen and A. Roy, Precision Measurement of the Casimir Force from 0.1 to 0.9 μm , *Phys. Rev. Lett.* **81**, 4549 (1998).
 - [20] Y. J. Chen, W. K. Tham, D. E. Krause, D. López, E. Fischbach and R. S. Decca, Stronger Limits on Hypothetical Yukawa Interactions in the 30–8000 nm Range, *Phys. Rev. Lett.* **116**, 221102 (2016).
 - [21] A. A. Geraci, S. J. Smullin, D. M. Weld, J. Chiaverini and A. Kapitulnik, Improved constraints on non-Newtonian forces at 10 microns, *Phys. Rev. D* **78**, 022002 (2008).
 - [22] D. J. Kapner, T. S. Cook, E. G. Adelberger, J. H. Gundlach, B. R. Heckel, C. D. Hoyle, and H. E. Swanson, Tests of the Gravitational Inverse-Square Law below the Dark-Energy Length Scale, *Phys. Rev. Lett.* **98**, 021101 (2007).
 - [23] A. A. Geraci, S. B. Papp, and J. Kitching, Short-Range Force Detection Using Optically Cooled Levitated Micro-

- spheres, *Phys. Rev. Lett.* **105**, 101101 (2010).
- [24] J. Liu and K. D. Zhu, Nanogravity gradiometer based on a sharp optical nonlinearity in a levitated particle optomechanical system, *Phys. Rev. D* **95**, 044014 (2017).
- [25] J. J. Li and K. D. Zhu, All-optical mass sensing with coupled mechanical resonator systems, *Phys. Rep.* **525**, 223 (2013).
- [26] P. Verlot, A. Tavernarakis, T. Briant, P. F. Cohadon, and A. Heidmann. Backaction Amplification and Quantum Limits in Optomechanical Measurements. *Phys. Rev. Lett.* **104**, 133602 (2010).
- [27] M. Aspelmeyer, T. J. Kippenberg, and F. Marquardt, Cavity optomechanics, *Rev. Mod. Phys.* **86**, 1391 (2014).
- [28] J. D. Thompson, B. M. Zwickl, A. M. Jayich, F. Marquardt, S. M. Girvin and J. G. E. Harris, Strong dispersive coupling of a high-finesse cavity to a micromechanical membrane, *Nature* **452**, 72–75 (2008).
- [29] R. S. Decca, D. López, H. B. Chan, E. Fischbach, D. E. Krause, and C. R. Jamell, Constraining New Forces in the Casimir Regime Using the Isoelectronic Technique *Phys. Rev. Lett.* **94**, 240401 (2005).
- [30] K. L. Ekinci, Y. T. Yang and M. L. Roukes, Ultimate limits to inertial mass sensing based upon nanoelectromechanical systems, *J. Appl. Phys.* **95**, 2682 (2004).